Chapter 6
Phosphorescence Lifetime Imaging (PLIM): State of the Art and Perspectives

Pavel S. Chelushkin and Sergey P. Tunik

Abstract This chapter reviews the status and perspectives of phosphorescence lifetime imaging (PLIM), an advanced imaging strategy that relies on phosphorescence lifetime measuring as a function of some particular biological microenvironment parameters. PLIM should be regarded as a functional imaging technique, as opposite to various forms of "localization" techniques, because it provides not only information on distribution pattern of the probe but also determines its "status" (via lifetime reporting).

6.1 Introduction

Luminescence imaging methods are among the most indispensable tools in the biosciences nowadays since they provide a unique combination of sensitivity and resolution in live experiments. The most common probes for luminescence imaging are fluorophores, singlet emitters featuring short lifetimes (0.1–10 ns) and small Stokes shifts (<100 nm) that results in strong interference of their emission with autofluorescence of the endogenous emitters. On the contrary, the triplet (phosphorescent) emitters based on luminescent transition metal complexes display both longer lifetimes (up to milliseconds) and larger Stokes shifts (>100 nm) that pave the way to efficient separation of their signals from background fluorescence. This improvement in signal-to-noise ratio is of particular importance for intensity measurement mode widely used in luminescent microscopy. However, application of this mode in quantitative measurements is considerably restricted because of uneven spatial distribution of the probe across the sample under study and uncertainty in emitting light intensity due to variations in media absorption characteristics.

P. S. Chelushkin · S. P. Tunik (✉)
Institute of Chemistry, St. Petersburg State University, Universitetskii pr., 26, Saint Petersburg 198504, Russia
e-mail: sergey.tunik@spbu.ru

P. S. Chelushkin
e-mail: p.chelushkin@spbu.ru

K. Yamanouchi et al. (eds.), *Progress in Photon Science*, Springer Series in Chemical Physics 119, https://doi.org/10.1007/978-3-030-05974-3_6

Application of lifetime-based techniques, referred to as fluorescence (FLIM) and phosphorescence (PLIM) lifetime imaging, makes possible to use the lifetime as a function of some particular biologically relevant microenvironment parameters. Thus, FLIM and PLIM should be regarded as "functional imaging" techniques, as opposite to various forms of "localization" imaging, because they provide not only information on distribution pattern of the probe in the sample but also determine its "status" (via reporting of lifetime).

While FLIM is a well-established part of modern biomedical studies [1, 2], its cognate, PLIM, is just an emerging area [3]. In this Perspective review, we will highlight the cutting edge research which use this method, without intention to cover exhaustively all the existing literature on PLIM, and present our vision of the prospectives of further development in this area with special focus on novel generations of PLIM probes and sensors.

6.2 State of the Art in PLIM Research

As for any other advanced bioimaging techniques, the overall progress in PLIM is a result of mutual synergistic stimulation of at least three areas of knowledge (Fig. 6.1), namely, physics (development of instrumentation and data treatment), chemistry (synthesis of advanced probes), and biomedicine (formulation of acute research directions and development of relevant models). Progress in a particular field opens up novel horizons and poses challenging requirements for the other fields thereby stimulating the overall progress. We will briefly describe in this section state of the art for each of the above fields; for historical survey of PLIM, the reader is referred to [4].

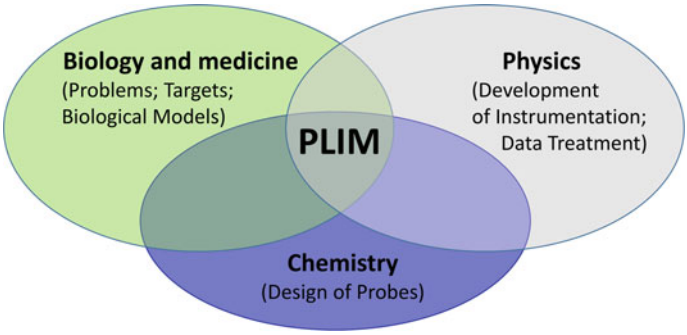

Fig. 6.1 Representation of PLIM as a multidisciplinary research area

6.2.1 PLIM Instrumentation: Confocal PLIM with TCSPC

To date, the most established approach for PLIM implementation is the use of raster scanning (confocal) technique accompanied with time-correlated single photon counting (TCSPC). Despite several promising alternatives (such as wide-field TCSPC PLIM [5] or frequency-domain PLIM [6] that can be performed on commercially available "LIFA-X" instrument from Lambert Instruments BV, Netherlands) this technique suggests at least two key advantages: (i) confocal scanning provides improved axial resolution inaccessible by wide-field techniques, and (ii) well established TCSPC data acquisition mode [7] makes possible robust and precise lifetime measurements compared to frequency-domain approaches although comes short in acquisition rate.

The up-to-date TCSPC FLIM/PLIM microscopy is described in detail elsewhere [8]; herein we briefly outline the essence of the routine. To collect the phosphorescence photons and emission decay of the probe molecules, the sample is scanned pixel-by-pixel, and during the pixel dwell time, the phosphors are first pumped by a high-frequency pulsed laser (the "laser ON" period); the laser is then switched off (the "laser OFF" period), phosphorescence photons are collected, and lifetime distribution is built up (Fig. 6.2a). Notably, the process described above allows simultaneous implementation of FLIM experiment by analyzing the distribution of the fluorescent photons during the "laser ON" period i.e. FLIM and PLIM data can be obtained simultaneously within the same acquisition time (Fig. 6.2b). Using of pulse train instead of single pulse for pumping the phosphorescence is highly advantageous since it maintains high sensitivity while decreasing photo damage and some undesirable processes (such as pile-up effect and detector overload) [8].

Thus, the combined TCSPC FLIM/PLIM experiment simultaneously provides information on the characteristics of fluorophores and phosphors presented in the object studied, it enables correlative mapping of metabolic information (so-called "optical redox ratio" [9], which measures ratio between flavin adenine dinucleotide, FAD, and nicotinamide adenine dinucleotide, NADH), and oxygen distribution derived from luminescence quenching of exogenous phosphorescent probe such as ruthenium tris-(2,2′-bipyridyl) dichloride [10], or covalent conjugates of human serum albumin with Pt(2-phenylpyridine)(triphenylphosphine)Cl complex that exerts "luminescence switch-on" effect via selective binding to histidine residues [11].

The raster scanning TCSPC approach can be extended to the macroscopic TCSPC PLIM. Moreover, confocal PLIM macro scanners (for example, "DCS-120 MACRO", Becker and Hickl, GmbH, Germany) have recently become commercially available. Nevertheless, there are only a few reports on the confocal macroscopic TCSPC PLIM to date [12, 13].

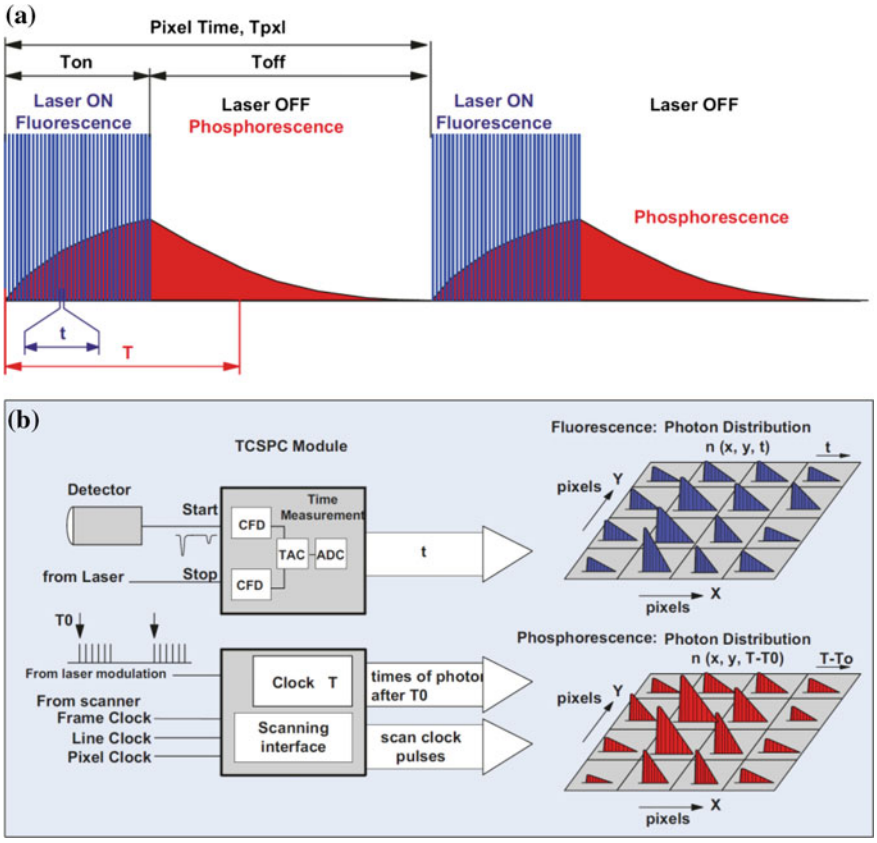

Fig. 6.2 Principle of simultaneous FLIM/PLIM with TCSPC. **a** Modulation scheme: a high-frequency pulsed laser is on-off modulated synchronously with the pixels. FLIM is recorded in the "Laser ON" phases, PLIM in the "Laser OFF" phases. **b** Scheme of simultaneous determination of fluorescence and phosphorescence lifetime distributions. Reprinted with permission from [8]. Copyright 2017 Springer

6.2.2 Biomedical Models

To date, PLIM was used for the variety of biomedical models, including monolayer cell cultures [10, 11], 3D tissue models (cell spheroids and organoids [14]), and living organisms (small animals [15]). In the case of 2D and 3D cell cultures (as well as in the case of in vivo microscopy) confocal TCSPC PLIM (or its FLIM/PLIM version) is the method of choice. In the case of macroscopic PLIM, to date the majority of studies were carried out using the wide-field macroscopic instruments that lack spatial resolution [15]. We believe that dissemination of confocal PLIM macro scanners mentioned above will change this area and eventually will lead to high-resolution in vivo PLIM.

6.2.3 *Probes for Practical PLIM*

Numerous phosphorescent probes designed for various PLIM applications have been described to date [3], but only one class of these compounds, namely, O_2 PLIM sensors, have been developed into commercial products applicable for oxygen mapping in biological samples. There are two major properties of the phosphorescent emitters, which made possible to use them as O_2 sensors in PLIM mode. The first one is that the excited state of phosphorescent compound and ground state of molecular oxygen are triplets that allows for energy transfer from excited state of the phosphor to O_2 molecule thus quenching the emission of triplet probes. Because the quenching is a dynamic process, it changes phosphorescence lifetime, making these probes excellent candidates for O_2 sensing by PLIM. The second reason consists in a relatively easy design of the probes with the combination of strong lifetime response onto oxygen concentration and minor dependence on other environment variables, including pH, temperature, interactions with proteins, etc.

To date, two approaches for the design of practically applicable PLIM O_2 sensors have been elaborated, which combine high lifetime sensitivity and selectivity with respect to oxygen. The first one was developed by Prof. D. Papkovsky's group and consists in solubilization of hydrophobic organometallic PLIM sensors (various platinum porphyrins, e.g. Pt(II)-*meso*-tetrakis(pentafluorophenyl)porphyrin, PtPFPP, Fig. 6.3) through their incorporation into nanoparticle-forming polymers (for example, cationic polymer Eudragit RL-100, Fig. 6.3) [16]. The resulting nanosensors (e.g. $NanO_2$, Fig. 6.3) easily penetrate into cells in 2D and 3D cell cultures, but are hardly applicable for whole-body in vivo imaging since (i) systemic administration of $NanO_2$ is doubtful because opsonization and phagocytosis caused by positive net charge of sensor nanoparticles [17–19] lead to accumulation cationic nanosensors in liver [20] and (ii) excitation wavelengths of $NanO_2$ (excitation maximum at 395 nm) are far from the first window of transparency of biological tissues (650–900 nm [21]).

The second approach was developed by Prof. Vinogradov's group and includes dendronization of Pd- (referred to as "Oxyphors" [15, 22], Fig. 6.4) or Pt-porphyrins [23, 24] with subsequent modification by polyethylene glycol (PEG) arms. PEGylation is prone to endow macromolecules with prolonged circulation in blood [25]. Though being cell-impermeable and thus inapplicable for intracellular oxygen mea-

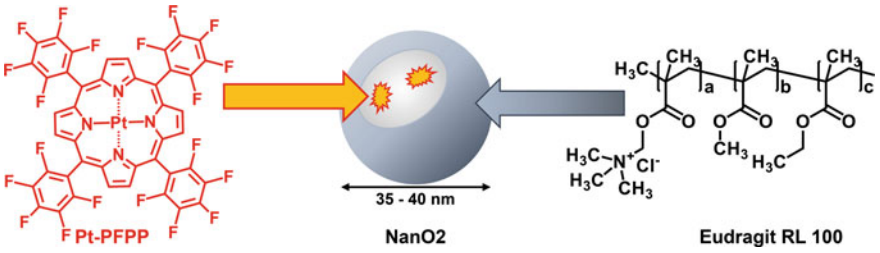

Fig. 6.3 Schematic structure of $NanO_2$ oxygen nanosensor described in [16]

surements, "Oxyphors" and related sensors are suitable for systemic administration and consequently promising for in vivo oxygenation measurements [15, 22].

The both approaches are based on essentially similar Pt/Pd-porphyrin emitters, which demonstrate phosphorescence in NIR area of the spectrum, display strong response to oxygen concentration and are rather insensitive to variations in temperature and pH. Additionally, the outer polymer "shell" (either polymer nanoparticle or branched dendrons) provides steric protection of the luminescent center from interaction with biomolecules, which may considerably and uncontrollably change the probe sensitivity to oxygen. However, this type of protection does not eliminate phosphor's sensitivity to oxygen since O_2 molecule is small enough to easily diffuse through the protective polymeric "shell" and get in contact with the triplet chromophore.

Nevertheless, in the context of increasing PLIM potential for in vivo imaging (*vide supra*) further tuning of photophysical and physico-chemical properties of prospective probes is highly desirable. Several key ideas have already been realized. The first one consists in variations in the structure and composition of metal porphyrins, e.g. in development of the porphyrine aromatic system, which may shift excitation and emission wavelengths into the first window of transparency of biological tissues (650–900 nm). As an example, the structure of Pd-tetrabenzoporphyrins [15] is presented in Fig. 6.4, which differs from standard porphyrin core (drawn by red color) by its conjugation with four benzo-groups (drawn by green color). This idea has led to several near-infrared sensors, including "NanO_2-IR" (Excitation/Emission wavelengths are 615/760 nm [26]) and "Oxyphor G4" (Excitation/Emission wavelengths are 637/813 nm [15]), and enabled whole-body tumor hypoxia imaging [15]. Unfortunately, excitation bands of the above probes still do not exactly fall into the window of transparency of biological tissues, and, to the best of our knowledge, there are no phosphors with one-photon excitation wavelength over 650 nm.

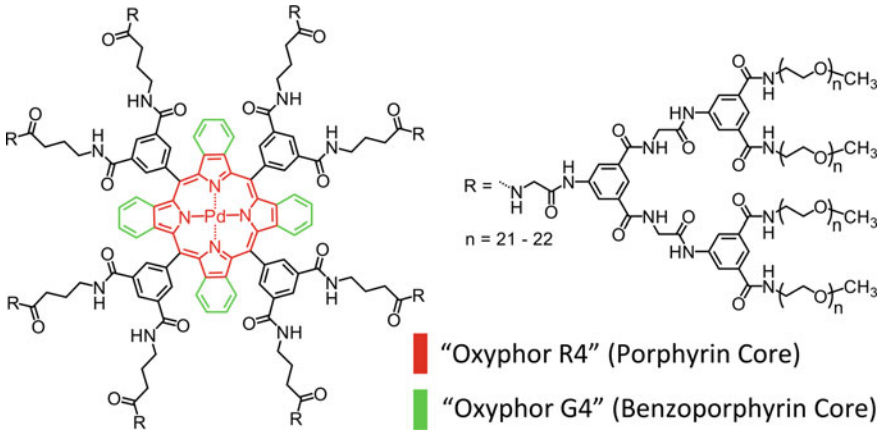

Fig. 6.4 Chemical structures of Oxyphors R4 and G4 described in [15]

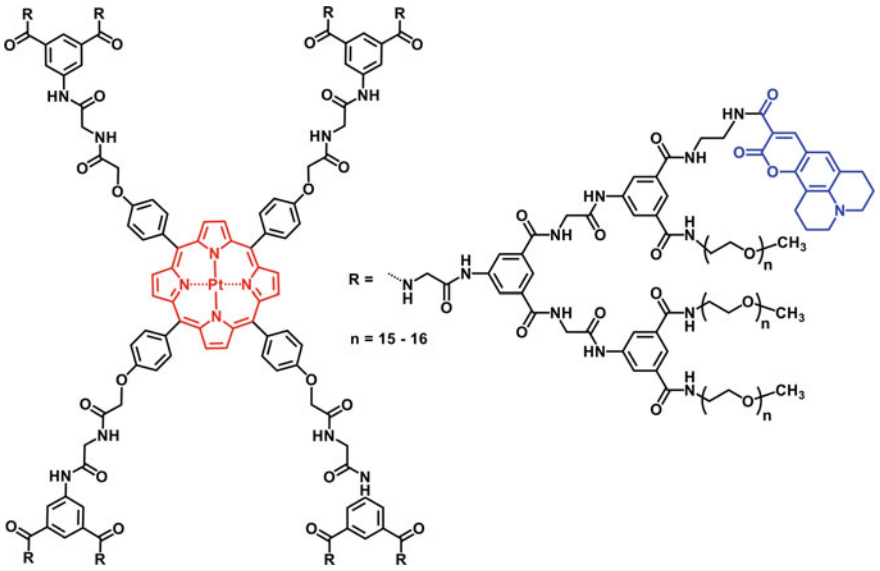

Fig. 6.5 Chemical structure of two-photon PLIM oxygen sensor—platinum porphyrin-coumarin-343 described in [23] and used in [28, 29] (see Fig. 6.6). Two-photon absorbing antenna (Coumarin 343) is depicted by blue, phosphorescent acceptor (Pt porphyrin core) is depicted by red color

The second improvement consists in the synthesis of molecular ensembles containing triplet chromophore with the excitation spectrum fit in the 350–500 nm range and two-photon absorbing antenna excited by femtosecond lasers operating at the wavelengths from 700 to 1000 nm, see Fig. 6.5. Two-photon antenna excitation followed by the resonance energy transfer to the triplet emitter gives resulting emission above 650 nm. In this case both excitation and emission fall into the first window of transparency of biological tissues. This approach requires extremely high density of photon flux, which is a major drawback of the probes of this type, because high light scattering in biological tissues makes it highly diffuse at the depths higher than 1 mm and inapplicable for multiphoton confocal experiments [21]. Consequently, in vivo use of this type of oxygen sensors is restricted to the measurements at depth not exceeding 1 mm [27].

Nevertheless, several two-photon O_2 sensors were developed either via covalent bonding of two-photon absorbing antenna (Coumarin 343, [23]; Coumarin 307, [24]) to PEGylated shell of Pt porphyrins (platinum analogs of "Oxyphors") or via simultaneous incorporation of two-photon antennas (polyfluorene) and Pt-porphyrins into either cationic nanoparticles made of Eudragit RL-100 (MM2 [30]) or anionic poly(methyl methacrylate-*co*-methacrylic acid) nanoparticles, referred to as PA2 [31]. Application of these sensors enabled direct in vivo measurements of local O_2 concentration in the bone marrow through the intact animals skull [28] (Fig. 6.6a), as well as high-resolution measurements of O_2 partial pressure in cerebral vasculature of animals (Fig. 6.6b) [29].

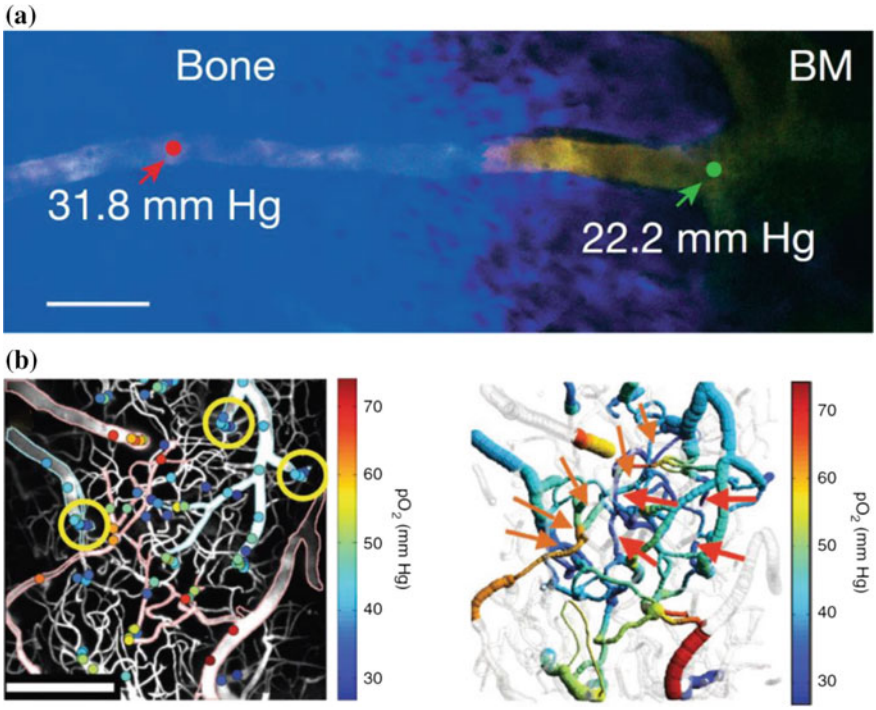

Fig. 6.6 Examples of in vivo two-photon PLIM oxygen sensing of platinum porphyrin-coumarin-343 (see Fig. 6.5 for structure). **a** Maximum intensity projection image montage of a blood vessel entering the bone marrow (BM) from the bone. Bone (blue) and blood vessels (yellow) are delineated with collagen second harmonic generation signal and Rhodamine B—dextran fluorescence, respectively. The two arrows point to locations of pO_2 measurements just before and after the vessel enters the BM. Scale bar: 100 μm. Reprinted with permission from [28]. Copyright 2014 Nature Publishing Group. **b** Measurement of pO_2 in cortical microvasculature. Left: measured pO_2 values in microvasculature at various depths (colored dots), overlaid on the maximum intensity projection image of vasculature structure (grayscale). Digital processing was performed to remove images of the dura vessels. Edges of the major pial arterioles and venules are outlined in red and blue, respectively. Right: composite image showing a projection of the imaged vasculature stack. Red arrows mark pO_2 measurement locations in the capillary vessels at 240 μm depth. Orange arrows point to the consecutive branches of the vascular tree, from pial arteriole (bottom left arrow) to the capillary and then to the connection with ascending venule (top right arrow). Scale bars: 200 μm. Reprinted with permission from [29]. Copyright 2010 Nature Publishing Group

Another prospective way to obtain the NIR excitation/emission probes consists in the use of up-converting antenna instead of two-photon one. This approach also allows shifting of both excitation and emission maxima into the first window of transparency, but, contrary to the previous case, excitation of up-converting antenna requires much less intense laser power and can be used for deep in vivo imaging. Despite the high promising potential of this approach, only a few publications have

described this method [32, 33], with only one example of PLIM oxygen imaging by up-converting sensors [32].

In conclusion, the most advanced to date application of PLIM is sensing of oxygen and imaging of its distribution in biological samples. A limited amount of probes based on the Pt/Pd porphyrins have found practical application in biomedicine; their derivatives containing tetra-benzoporphyrins as emitters and either two-photon or up-converting antennae display excitation and emission wavelengths in the windows of transparency of biological tissues that makes them applicable for in vivo microscopic experiments.

6.3 Perspectives of PLIM

As mentioned above, the general progress of PLIM is a result of mutual synergistic influence of at least three major research areas, including development of instrumentation, biological models, and phosphorescent probes.

In the field of instrumentation, we believe that further progress will focus on implementation of more affordable instruments, which will provide shorter acquisition times (now typical PLIM experiment takes from minutes to tens of minutes) accompanied by enhanced spatial resolution. This could be achieved via optical schemes allowing more efficient photon harvesting, using multiple detectors, etc.

In the field of biological models, on the one hand, new animal models are being intensely developed, especially in the areas of neuro- and cancer imaging; so PLIM techniques must progress concurrently to match requirements of new objects to be studied. The ultimate goal in this area is performing of single cell visualization within living and intact body [34]. On the other hand, more sophisticated cell constructs are evolved, and increasing tendency of switching from 2D and "quasi-uniform" (i.e. consisting of one cell type) 3D models, to highly differentiated 3D tissue models including "organoids" and artificially engineered tissues. Reference [14] presents excellent recent overview of implementation and perspectives of PLIM and related imaging techniques in the field of 3D tissue modelling.

The progress in the above-mentioned fields is definitely posing novel challenges for the development of phosphorescent probes compatible with requirements of biomedical experiments (solubility and stability in physiological media, biocompatibility, retaining of sensitivity to analytes in biological samples) and best suitable for effective acquisition of the data in lifetime domain. Below we will highlight the main challenges and emerging areas of design and development of phosphorescent probes.

6.3.1 Non-oxygen Sensing

The most obvious idea in this field is application of PLIM for sensing of various microenvironment parameters (such as pH, temperature, ionic strength) and biologically relevant analytes other than oxygen (cations/anions, biothiols etc.). The latter area includes but not limited to development of sensors to low molecular ions (Zn^{2+}, Cl^-, F^-, ClO^-), biologically important molecules (including H_2S, cysteine as well as other biothiols, DNA, miRNA, etc.) and selective stains for different organelles (nucleus, nucleoli, mitochondria, lysosomes, and cell membrane). The key achievements in bioanalytics of this sort are exhaustively reviewed in the recent publication [3], however neither of these probes have become a commercial product yet. One of possible explanations (in addition to exceptional youth of this area) is that, contrary to oxygen sensor, other sensors and trackers do not possess such a robust and unambiguously interpretable lifetime correlations with appropriate analytes (as it was achieved in the case of oxygen sensing) and often display concomitant lifetime dependence on other microenvironment characteristics.

Two possible strategies may be used to decouple/avoid the cross-talk between target and obstructive parameters and to design effective non-oxygen PLIM sensors. The first strategy consists in rational design of the probe architecture (choice of appropriate luminescent center and ligand environment selectively responsive to the target analytes) while the other one should be based on embedding of phosphors into responsive matrix (various kinds of nanoparticles, conjugation to polymers, etc.). Below (in the rest of this Section) we describe both approaches in detail.

6.3.1.1 Rational Design of Phosphor Architecture

Molecular thermometers. One of the challenging tasks in functional bioimaging is preparation of PLIM molecular sensor with lifetime response onto temperature variations in physiological interval. The design of this type of probes relies on the recent findings of strong luminescence intensity [35] and lifetime [36] dependence of europium complexes on temperature within the 30–45 °C range. Moreover, the europium compounds luminescence was found to be nearly independent of oxygen concentration that allows avoiding cross-talking of these physiological parameters. Consequently, europium complexes are very attractive candidates for PLIM temperature sensing. For example, Eu-tris(dinaphthoylmethane)-bis-(trioctylphosphine oxide) complex (Fig. 6.7a) incorporated into poly(methyl methacrylate)-based nanoparticles demonstrated variations of luminescence lifetime from 230 to 170 μs in response to the temperature increase from 30 to 40 °C [36]. Though these PLIM experiments were restricted to investigation of sensor nanoparticles embedded into poly(vinyl alcohol) films [36], this example demonstrates high potential of Eu complexes in temperature tracking in biological samples, e.g. in living cells, in response to stimuli of various nature, using PLIM technique. Aside from Eu complexes, various nanomaterials, such as silicon nanoparticles [37] or gold nan-

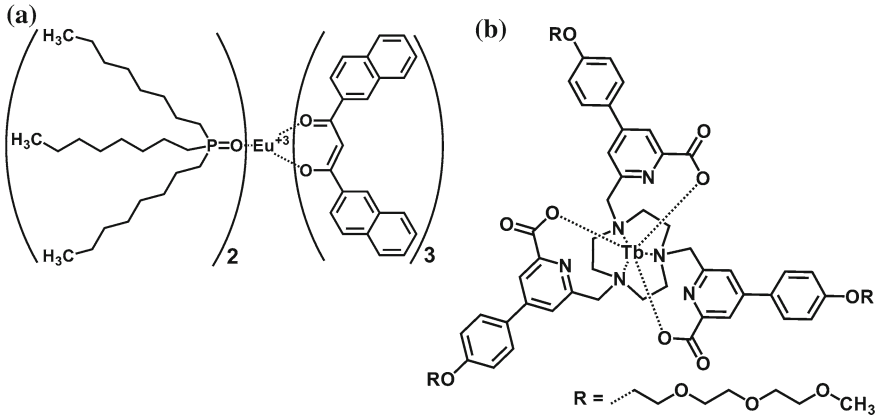

Fig. 6.7 Structures of **a** Eu(III) thermometer described in [36] and **b** Tb(III) viscometer described in [39]

oclusters [38], also demonstrate substantial lifetime temperature dependences and are promising for application as PLIM molecular thermometers.

Molecular viscometers. In the case of microviscosity measurements, an effective strategy consists in the development of probes bearing ligands with auxiliary rotors. In the case of correct design, the rotor's internal rotation can contribute into one of nonradiative relaxation channels. As a result, increase in microviscosity slows down internal rotation to give the decrease in nonradiative relaxation rate, and, ultimately, elongation of luminescence lifetimes and increase in luminescence intensity. This concept was exemplified by Tb(III) complex bearing biaryl rotors (Fig. 6.7b) that exhibited statistically significant increase in lifetimes within the nuclei compared to the cytoplasm [39].

Molecular pH meters. Incorporation of protonatable groups into ligands of phosphorescent complexes renders them pH sensitive. For example, two Ir(III) complexes bearing N,N ligands featuring β-carboline motif (Fig. 6.8) displayed both pH dependence and accumulation in lysosomes as a result of secondary amino group protonation [40]. The complexes are thus regarded as promising pH sensors though their sensitivity to oxygen quenching and interaction with lysosomal constituents should be investigated to avoid potential misinterpretations of lifetime changes.

6.3.1.2 Polymer-Based Environmentally Responsive Sensors

An alternative idea of sensors development consists in the use of phosphor conjugates with environmentally responsive polymers. This approach was successfully exemplified by molecular thermometer based on the conjugate of luminescent iridium complexes with thermally responsive polymer [41]. The polymer undergoes conformational coil-to-globule transition in physiological temperature range that results

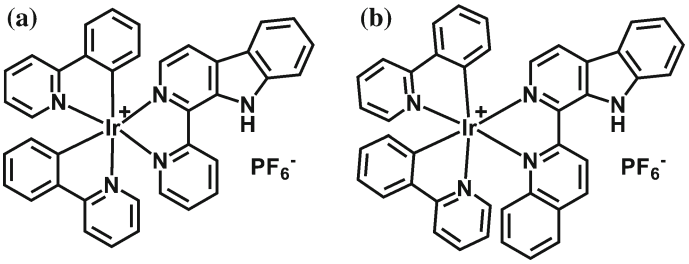

Fig. 6.8 Structures of pH-sensitive Ir(III) complexes described in [40]

in dramatic change in luminescence intensity. This approach was implemented in both ratiometric and PLIM imaging modalities for temperature measurements, but generally this idea can be broadened to other microenvironment parameters such as pH, ionic strength, and viscosity provided that at least two requirements were met. First, luminescent complex should be as little as possible environmentally sensitive by itself. Second, the core-shell architecture with environmentally responsive core conjugated with the phosphor and hydrophilic outer shell that sterically protects labels from unwanted interactions seems to be more preferable compared to linear polymers.

6.3.2 Towards Live Imaging of Cell/Tissue Metabolism

Another growth point in the PLIM research will be the switching from "concentration measurement" to "metabolic" imaging, i.e. obtaining of information on the status of organelle, cell or tissue rather than just quantitative imaging of the distribution of oxygen or other analytes. In fact, such metabolic imaging has already been implemented in FLIM, where the "optical redox ratio", the term encompassing ratios between free and protein-bound NADH (electron donor) and FAD (electron acceptor), directly calculated from FLIM, is intensely investigated and was proved to differentiate between normal and precancerous cells [9]. In analogy to the above term, we believe that it is possible to design PLIM probes, which would respond to some metabolic shifts or processes by corresponding changes in lifetimes. To date, there is no clear understanding of what kind of metabolic response could be used for such analysis but we would highlight several emerging applications that have the potential of transformation into metabolic imaging.

The first of these examples is the real-time sensing of newly synthesized proteins [42]. To realize this analytical instrument, the authors first forced cells to produce proteins with methionine substituted by L-azidohomoalanine (AHA), the methionine structural analog, by incubating them in methionine-free media supplemented with AHA (Fig. 6.9a) [43]. The newly synthesized proteins contained azido groups and thus were able to conjugate with iridium complex containing alkynyl groups via

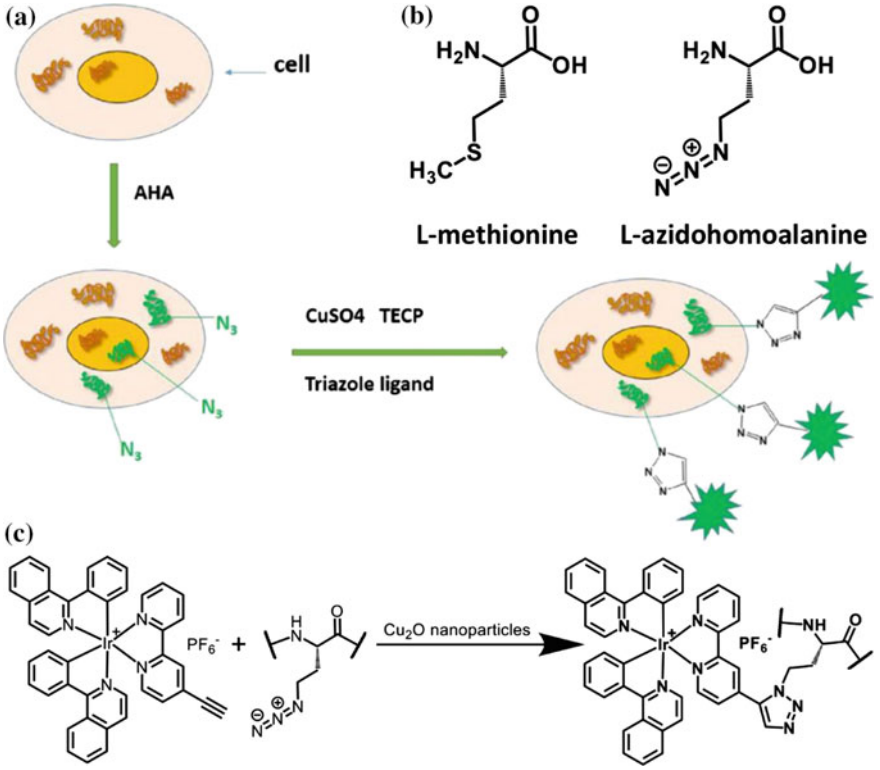

Fig. 6.9 Experimental scheme of bioorthogonal labelling of newly synthesized proteins for fluorescence visualization in cells. **a** Schematic diagram of metabolic labelling of newly synthesized proteins in mammalian cells using L-azidohomoalanine (AHA) incorporation and then over the Cu (I)-catalyzed [3+2] azide–alkyne cycloaddition to label fluorescence. Reprinted with permission from [43]. Copyright 2017 Elsevier. **b** Chemical structures of L-methionine and AHA. C. Scheme of click reaction between Ir-alkyne complex and AHA residue described in [42]

click reaction directly inside cells (Fig. 6.9b). Upon this conjugation the lifetime of iridium complex dramatically decreased from 600–800 (free complex) to 400–600 ns (conjugated complex) without variations in the energy of emission. As a result, monitoring of protein synthesis dynamics became possible. This example shows not only principal ability to perform selective bioconjugation inside living cells but also paves the way to the design of sensors with lifetime response onto changes in essential characteristics of biomolecules and organelles including complex formation or disintegration, dimerization, conformational changes, etc.

In this context, metabolic DNA imaging looks particularly attractive. DNA is the molecule that undergoes substantial conformational transitions during cell cycle, and elaboration of PLIM sensors changing their lifetimes in response to DNA compaction/unfolding would eventually lead to creation of "PLIM cell cycle clocks". To date, such complexes are not found yet, though there are some significant results

obtained in closely related area. The most promising example consists in development of dinuclear ruthenium "light-switch" DNA probes [44] (Fig. 6.10a). These complexes demonstrate strong luminescence enhancement accompanied by almost two-fold increase in lifetimes upon interaction with DNA but, unfortunately, do not show any significant lifetime variations during DNA transformations characteristic for different cell cycle stages. Nevertheless, other chemistry can be offered to gain desirable lifetime sensitivity, and using of chiral isomers would be advantageous in this context, since DNA is also chiral molecule, and this hypothesis is corroborated in part by demonstration of the fact that interaction of DNA with Δ and Λ enantiomers of another (but similar) ruthenium complex resulted in substantially different lifetimes [45] (Fig. 6.10b).

Analogously to the above example related to DNA, metabolic PLIM imaging can be adapted for other biologically relevant biomolecules, as well as to cell compartments (e.g., inner or outer membranes) or even organelles, such as mitochondria, lisosomes, Golgi apparatus, adiposomes, etc. Despite numerous reports on organelle-specific phosphors, there are only a few attempts to evaluate applicability of these probes in PLIM. Potential metabolic sensors may respond to different stimuli such as variations on redox potential or degree of membrane polarization, activation/inhibition of proteases, esterases, or any other ferments, polarity, etc.

For example, we have shown [46] that lipohilic homoleptic Au-alkynyl cluster (Fig. 6.11a) demonstrates rather unexpected behavior in lipid droplets. While distributing rather uniformly between lipid droplets (based on intensity measurements; Fig. 6.11b), the complexes demonstrate two distinct domains in lifetime distribution (Fig. 6.11c–d), with one lifetime drastically different from that observed in model lipid media (vegetable oil) [46]. Though there is no experimentally supported explanation of the appearance of the additional lifetime mode, this observation clearly shows advantageous nature of PLIM functional imaging over usual "localization"

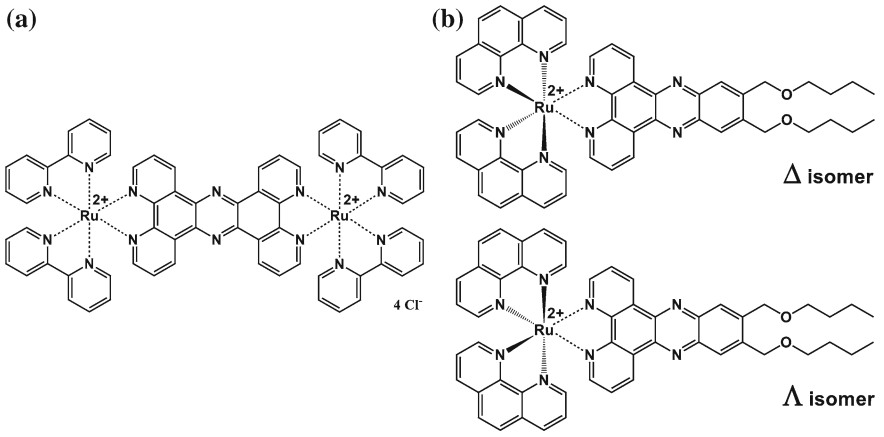

Fig. 6.10 Chemical structures of Ru complexes described in [44] (**a**) and [45] (**b**)

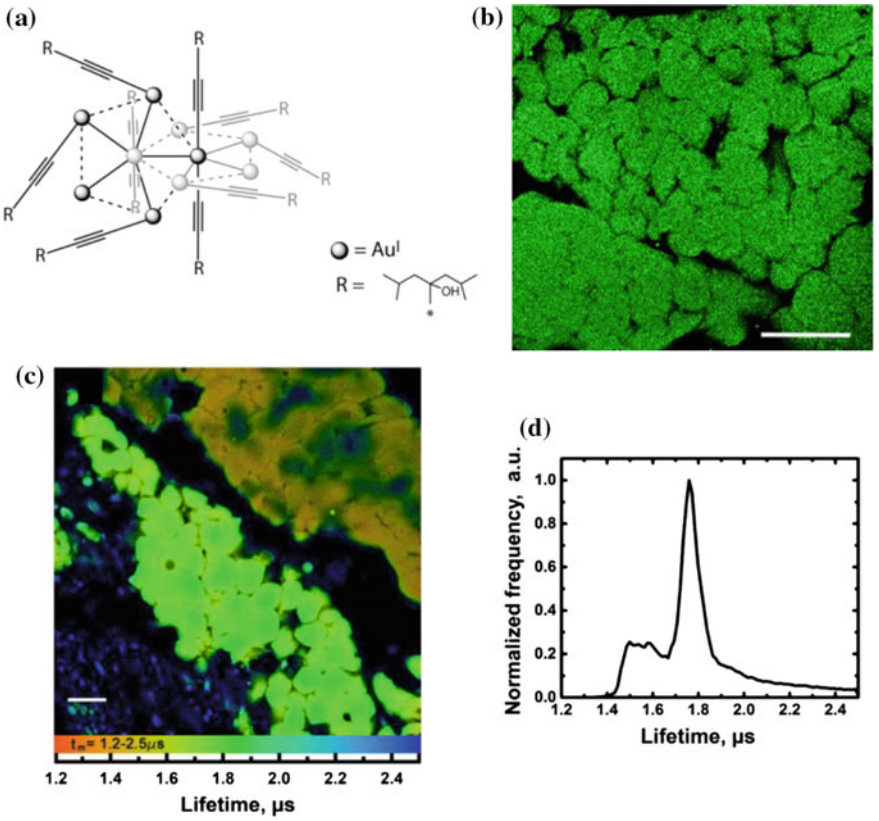

Fig. 6.11 **a** Schematic structure of lipophilic Au cluster. Visualization of adipocytes in the chicken subcutaneous adipose tissue (**b**, **c**): **b** Signal detection with spectral imaging. **c** Phosphorescence lifetime image. **d** Distribution of the phosphorescence lifetimes across the image (**c**). Two-photon excitation at 710 nm. Scale bar: 100 µm. Reproduced with permission from [46]. Copyright 2017 Elsevier

mode: in addition to visualization and "localization" of cell compartments provided by both modalities, functional imaging also provides information on the "status" of the region of interest, provided that there is an unambiguous correlation between the specific environmental property and lifetime.

6.3.3 Dual (Ultimately—Multiple) Sensors

Another approach that seems to be developed rapidly in the nearest future is elaboration of dual emission probes, which could perform simultaneous sensing of two independent parameters for correlative mapping. In a remote perspective multiple

sensors have a clear prospective to become an advanced tool in functional bioanalytics. In the case of dual sensors, two principal constructions can be offered.

6.3.3.1 Dual-Modality FLIM/PLIM Probes

As it was demonstrated above (Sect. 6.2.1), modern PLIM equipment allows parallel performing of PLIM and FLIM measurements. Consequently, it is natural to suppose that dual emission fluorescent-phosphorescent probe would be an ideal candidate for simultaneous FLIM/PLIM experiment. This candidate should meet the following requirements: (i) excitation bands of both luminophores should overlap to make possible simultaneous excitation; (ii) emission band of the fluorophore should not overlap with excitation band of phosphor to avoid self-quenching; (iii) lifetimes of both probes should demonstrate a wide dynamic range in response to two mutually orthogonal microenvironment changes within physiological interval.

To date, despite numerous papers describing dual emission fluorescent-phosphorescent constructions, there was no reports on their application in dual FLIM/PLIM sensing mode: the overall majority of such dual probes are used as ratiometric sensors for oxygen. The conceptually closest example to the above ideas was demonstrated in the work describing simultaneous FLIM/PLIM mapping of temperature and oxygen by two simultaneously administered sensors: the FLIM sensor on temperature and PLIM sensor on oxygen [47].

6.3.3.2 Dual and Multiple PLIM Probes

Since lifetime range characteristic of phosphorescent emitters and potentially applicable in PLIM is at least of 5 orders of magnitude (from 10^{-8} to 10^{-3} s; Fig. 6.12), simultaneous acquisition of lifetime information from several phosphors is possible. For example, Lakowicz and co-workers clearly demonstrated PLIM differentiation of three Ru complexes displaying rather close lifetimes (7, 17, and 42 ns for tris(5-amino-1,10-phenanthroline)ruthenium(II), tris(2,2′-bipyridine)ruthenium(II), and tris(2,3-bis(2-pyridyl)pyrazine))ruthenium(II), correspondingly) individually incorporated into silver nanoshells (SiO_2 nanoparticles covered by Ag nanolayer) [48]. Hence, upon appropriate intracellular targeting, simultaneous multi-tracker imaging is possible, with the number of trackers sufficiently exceeding currently available range of fluorescent ones (up to 4 species in FLIM mode; up to 6 species in spectral imaging mode). In the case of phosphorescent sensors working in much broader lifetime interval (up to 10-fold change of lifetime upon variation of analyte concentration) differentiation of at least four phosphors with lifetimes differing by at least one order of magnitude (e.g., 10–100 ns, 0.1–1, 1–10 and 10–100 μs) is possible.

Regarding the combination of several phosphors into one construction, several different Eu–Ir dual phosphors were involved in assessment of their applicability in PLIM to date (Fig. 6.13) [49–51]. Unfortunately, PLIM experiments were described

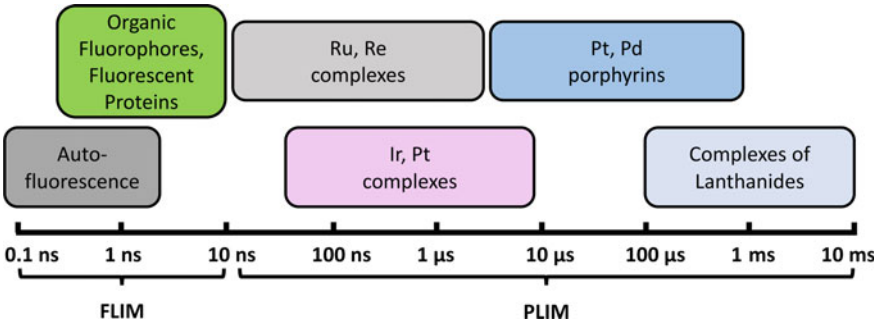

Fig. 6.12 Typical time intervals characteristic for FLIM and PLIM, and typical lifetimes of different classes of phosphors

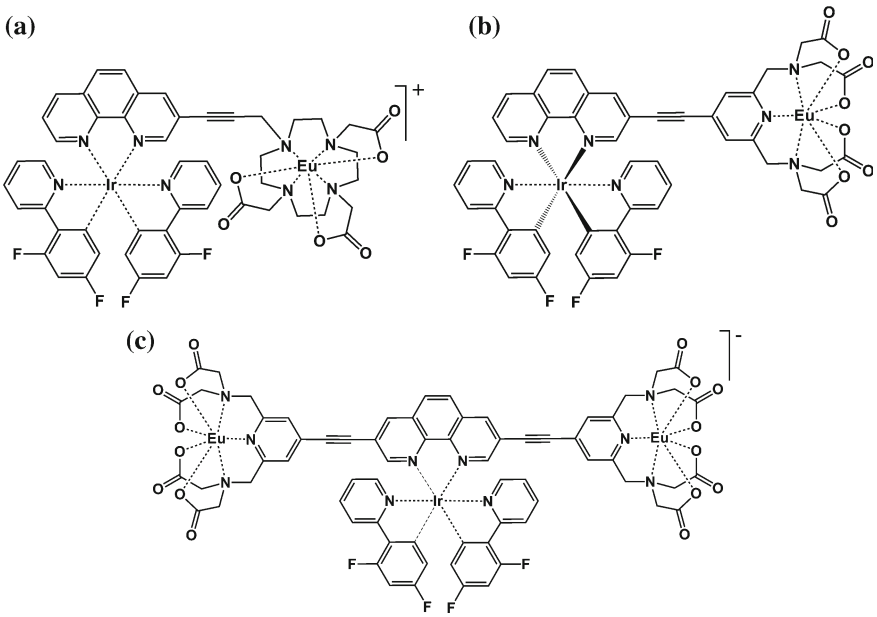

Fig. 6.13 Structures of dual Eu–Ir complexes described in [49] (**a**), [50] (**b**) and [51] (**c**), respectively

for Ir-based luminescence solely while Eu-based luminescence was used in time gating mode [49]. Most probably, this was because of a very long emission lifetimes of Eu chromophore that turned image acquisition time unacceptably long. Nevertheless, this approach seems to be very promising, and other luminophore combinations are anticipated.

6.4 Conclusions

In conclusion, this brief review is aimed to demonstrate that PLIM is an emerging and rapidly growing molecular imaging modality as well as to outline still unexplored areas of the method application. Contrary to the majority of molecular imaging modalities, PLIM is the functional imaging, i.e. it is the approach that visualizes not only distribution of a probe, but also its functional state in one or another way related to physiological status of the sample under study. Despite its relative youth, this approach has already become an important tool in the area of molecular imaging with the alternative and quite robust methodology of oxygen sensing/mapping. We envision that nearest future will see not only step-by-step progress in this area (i.e. improvement of equipment, sophistication of biomedical models, appearance of novel commercial probes and selective trackers suitable for PLIM) but also qualitative transition of PLIM to a new stage—the era of metabolic phosphorescence lifetime imaging.

Acknowledgements The authors greatly appreciate financial support from the Russian Science Foundation (grant 16-43-03003) and the organizing committee of the STEPS program for the support in publication of this review.

References

1. W. Becker, J. Microsc. **247**, 119 (2012)
2. M.Y. Berezin, S. Achilefu, Chem. Rev. **110**, 2641 (2010)
3. K.Y. Zhang, Q. Yu, H. Wei, S. Liu, Q. Zhao, W. Huang, Chem. Rev. **118**, 1770 (2018)
4. E. Baggaley, J.A. Weinstein, J.A.G. Williams, Struct. Bond. **165**, 205 (2015)
5. L.M. Hirvonen, K. Suhling, Meas. Sci. Technol. **28** (2017)
6. S.S. Howard, A. Straub, N.G. Horton, D. Kobat, C. Xu, Nat. Photonics **7**, 33 (2013)
7. W. Becker, *Advanced Time-Correlated Single Photon Counting Techniques* (Springer, Berlin, Heidelberg, 2005)
8. W. Becker, V. Shcheslavskiy, A. Rück, Adv. Exp. Med. Biol. 19–30, (2017)
9. M.C. Skala, K.M. Riching, A. Gendron-Fitzpatrick, J. Eickhoff, K.W. Eliceiri, J.G. White, N. Ramanujam, Proc. Natl. Acad. Sci. **104**, 19494 (2007)
10. S. Kalinina, J. Breymayer, P. Schäfer, E. Calzia, V. Shcheslavskiy, W. Becker, A. Rück, J. Biophotonics **9**, 800 (2016)
11. A.I. Solomatina, P.S. Chelushkin, D.V. Krupenya, I.S. Podkorytov, T.O. Artamonova, V.V. Sizov, A.S. Melnikov, V.V. Gurzhiy, E.I. Koshel, V.I. Shcheslavskiy, S.P. Tunik, Bioconjug. Chem. **28**, 426 (2017)
12. V. Shcheslavskiy, M. Shirmanova, V. Dudenkova, K. Lukyanov, A. Gavrina, A. Shumilova, E. Zagaynova, W. Becker, Opt. Lett. **43** (2018)
13. A.I. Solomatina, S.-H. Su, M.M. Lukina, V.V. Dudenkova, V.I. Shcheslavskiy, C.-H. Wu, P.S. Chelushkin, P.-T. Chou, I.O. Koshevoy, S.P. Tunik, RSC Adv. **8**, 17224 (2018)
14. R.I. Dmitriev (ed.), *Multi-Parametric Live Cell Microscopy of 3D Tissue Models* (Springer International Publishing, Cham, 2017)
15. T.V. Esipova, A. Karagodov, J. Miller, D.F. Wilson, T.M. Busch, S.A. Vinogradov, Anal. Chem. **83**, 8756 (2011)

16. A. Fercher, S.M. Borisov, A.V. Zhdanov, I. Klimant, D.B. Papkovsky, ACS Nano 5499–5508 (2011)
17. D.E. Owens, N.A. Peppas, Int. J. Pharm. **307**, 93 (2006)
18. S. Dufort, L. Sancey, J.L. Coll, Adv. Drug Deliv. Rev. **64**, 179 (2012)
19. F. Alexis, E. Pridgen, L.K. Molnar, O.C. Farokhzad, Mol. Pharm. 505–515 (2008)
20. R.I. Dmitriev, S.M. Borisov, H. Düssmann, S. Sun, B.J. Müller, J. Prehn, V.P. Baklaushev, I. Klimant, D.B. Papkovsky, ACS Nano **9**, 5275 (2015)
21. V. Ntziachristos, Nat. Methods **7**, 603 (2010)
22. I. Dunphy, S.A. Vinogradov, D.F. Wilson, Anal. Biochem. **310**, 191 (2002)
23. O.S. Finikova, A.Y. Lebedev, A. Aprelev, T. Troxler, F. Gao, C. Garnacho, S. Muro, R.M. Hochstrasser, S.A. Vinogradov, Chem. Phys. Chem. **9**, 1673 (2008)
24. E. Roussakis, J.A. Spencer, C.P. Lin, S.A. Vinogradov, Anal. Chem. **86**, 5937 (2014)
25. J. Milton Harris, R.B. Chess, Nat. Rev. Drug Discov. **2**, 214 (2003)
26. V. Tsytsarev, H. Arakawa, S. Borisov, E. Pumbo, R.S. Erzurumlu, D.B. Papkovsky, J. Neurosci. Methods **216**, 146 (2013)
27. F. Helmchen, W. Denk, Nat. Methods **2**, 932 (2005)
28. J.A. Spencer, F. Ferraro, E. Roussakis, A. Klein, J. Wu, J.M. Runnels, W. Zaher, L.J. Mortensen, C. Alt, R. Turcotte, R. Yusuf, D. Côté, S.A. Vinogradov, D.T. Scadden, C.P. Lin, Nature **508**, 269 (2014)
29. S. Sakadžić, E. Roussakis, M.A. Yaseen, E.T. Mandeville, V.J. Srinivasan, K. Arai, S. Ruvinskaya, A. Devor, E.H. Lo, S.A. Vinogradov, D.A. Boas, Nat. Methods **7**, 755 (2010)
30. A.V. Kondrashina, R.I. Dmitriev, S.M. Borisov, I. Klimant, I. O'Brien, Y.M. Nolan, A.V. Zhdanov, D.B. Papkovsky, Adv. Funct. Mater. **22**, 4931 (2012)
31. R.I. Dmitriev, S.M. Borisov, A.V. Kondrashina, J.M.P. Pakan, U. Anilkumar, J.H.M. Prehn, A.V. Zhdanov, K.W. McDermott, I. Klimant, D.B. Papkovsky, Cell. Mol. Life Sci. **72**, 367 (2015)
32. W. Lv, T. Yang, Q. Yu, Q. Zhao, K.Y. Zhang, H. Liang, S. Liu, F. Li, W. Huang, Adv. Sci. **2** (2015)
33. J. Liu, Y. Liu, W. Bu, J. Bu, Y. Sun, J. Du, J. Shi, J. Am. Chem. Soc. **136**, 9701 (2014)
34. T. Misgeld, M. Kerschensteiner, Nat. Rev. Neurosci. **7**, 449 (2006)
35. Y. Takei, S. Arai, A. Murata, M. Takabayashi, K. Oyama, S. Ishiwata, S. Takeoka, M. Suzuki, ACS Nano **8**, 198 (2014)
36. H. Peng, M.I.J. Stich, J. Yu, L.N. Sun, L.H. Fischer, O.S. Wolfbeis, Adv. Mater. **22**, 716 (2010)
37. Q. Li, Y. He, J. Chang, L. Wang, H. Chen, Y.W. Tan, H. Wang, Z. Shao, J. Am. Chem. Soc. **135**, 14924 (2013)
38. L. Shang, F. Stockmar, N. Azadfar, G.U. Nienhaus, Angew. Chemie Int. Ed. **52**, 11154 (2013)
39. A.T. Bui, A. Grichine, A. Duperray, P. Lidon, F. Riobé, C. Andraud, O. Maury, J. Am. Chem. Soc. **139**, 7693 (2017)
40. L. He, C.P. Tan, R.R. Ye, Y.Z. Zhao, Y.H. Liu, Q. Zhao, L.N. Ji, Z.W. Mao, Angew. Chemie Int. Ed. **53**, 12137 (2014)
41. Z. Chen, K.Y. Zhang, X. Tong, Y. Liu, C. Hu, S. Liu, Q. Yu, Q. Zhao, W. Huang, Adv. Funct. Mater. **26**, 4386 (2016)
42. J. Wang, J. Xue, Z. Yan, S. Zhang, J. Qiao, X. Zhang, Angew. Chemie Int. Ed. **56**, 14928 (2017)
43. J. Wang, L. Sheng, H. Zhao, X. Zhang, S. Zhang, Talanta **162**, 641 (2017)
44. E. Baggaley, M.R. Gill, N.H. Green, D. Turton, I.V. Sazanovich, S.W. Botchway, C. Smythe, J.W. Haycock, J.A. Weinstein, J.A. Thomas, Angew. Chemie Int. Ed. **53**, 3367 (2014)
45. F.R. Svensson, M. Abrahamsson, N. Strömberg, A.G. Ewing, P. Lincoln, J. Phys. Chem. Lett. **2**, 397 (2011)
46. E.I. Koshel, P.S. Chelushkin, A.S. Melnikov, P.Y. Serdobintsev, A.Y. Stolbovaia, A.F. Saifitdinova, V.I. Shcheslavskiy, O. Chernyavskiy, E.R. Gaginskaya, I.O. Koshevoy, S.P. Tunik, J. Photochem. Photobiol. A Chem. **332**, 122 (2017)
47. J. Jenkins, S.M. Borisov, D.B. Papkovsky, R.I. Dmitriev, Anal. Chem. **88**, 10566 (2016)

48. J. Zhang, Y. Fu, J.R. Lakowicz, J. Phys. Chem. C **115**, 7255 (2011)
49. E. Baggaley, D.K. Cao, D. Sykes, S.W. Botchway, J.A. Weinstein, M.D. Ward, Chem. A Eur. J. **20**, 8898 (2014)
50. A. Jana, E. Baggaley, A. Amoroso, M.D. Ward, Chem. Commun. **51**, 8833 (2015)
51. A. Jana, B.J. Crowston, J.R. Shewring, L.K. McKenzie, H.E. Bryant, S.W. Botchway, A.D. Ward, A.J. Amoroso, E. Baggaley, M.D. Ward, Inorg. Chem. **55**, 5623 (2016)